Journal of Power Sources 255 (2014) 151–156

Contents lists available at ScienceDirect

Journal of Power Sources

journal homepage: www.elsevier.com/locate/jpowsour

Parametric optimization of thermoelectric elements footprint for maximum power generation

A. Rezania [a,*], L.A. Rosendahl [a], H. Yin [b]

[a] Department of Energy Technology, Aalborg University, DK-9220 Aalborg, Denmark
[b] TEGnology ApS, DK-7100 Vejle, Denmark

HIGHLIGHTS

- Optimal footprint ratio of n- and p-type thermoelectric (TE) elements is explored.
- Maximum power generation and maximum cost-performance are achieved at $A_n/A_p < 1$.
- The model describes of the temperature distribution and voltage generation.
- The parametric optimization is considered for temperature dependent TE materials.
- Results are in a good agreement with the previous computational studies.

ARTICLE INFO

Article history:
Received 29 October 2013
Received in revised form
29 December 2013
Accepted 1 January 2014
Available online 8 January 2014

Keywords:
Thermoelectric uni-couple
Optimal footprint ratio
Maximum power generation
Heat transfer coefficient

ABSTRACT

The development studies in thermoelectric generator (TEG) systems are mostly disconnected to parametric optimization of the module components. In this study, optimum footprint ratio of n- and p-type thermoelectric (TE) elements is explored to achieve maximum power generation, maximum cost-performance, and variation of efficiency in the uni-couple over a wide range of the heat transfer coefficient on the cold junction. The three-dimensional (3D) governing equations of the thermoelectricity and the heat transfer are solved using the finite element method (FEM) for temperature dependent properties of TE materials. The results, which are in good agreement with the previous computational studies, show that the maximum power generation and the maximum cost-performance in the module occur at $A_n/A_p < 1$ due to difference in electrical resistance and heat conductivity of the considered materials.

1. Introduction

Novel technologies of electrical power generation which promise alternative green technology for fuel based energy sources, has been extensively researched in recent decades due to limitations of energy resource and in particular global warming [1]. Thermoelectric generators (TEGs) offer a very promising method to reclaim the large amount of available thermal energy into electricity. The development studies in TEG systems are mostly disconnected to the parametric optimization of the module components, and most of the works require a significant amount of engineering parametric analysis.

To increase the performance of the TE modules, most of research focused on development of TE materials to improve the dimensionless figure-of-merit (ZT) of the material [2]. Moreover, performance of TE modules has been modeled for various applications such as fuel cell system [3], automotive [4,5], spacing [6] etc.

Apart from the module design, co-design of the TE uni-couple in conjugation with the thermal boundary conditions can also play important role to improve the module performance for specific applications. There are few works that consider the effect of heat sink on the optimal geometry of TEG. Some studies [7,8] developed and utilized for parametric analysis of TE systems using an optimized analytic model. Although, these studies are in conjunction with the heat sink design but identical materials of TE elements are considered. The n- and p-type TE materials are not naturally identical. Different thermal conductivity of the materials causes different temperature distribution in the thermoelements. Since the electrical resistance and the Seebeck coefficient of the materials depend on temperature, the power factor of the n- and p-type

* Corresponding author.
E-mail address: alr@et.aau.dk (A. Rezania).

0378-7753/$ – see front matter © 2014 Elsevier B.V. All rights reserved.
http://dx.doi.org/10.1016/j.jpowsour.2014.01.002

Nomenclature

A	footprint area, m^2
$\vec{D}$	electric flux density vector, C m^{-2}
$\vec{E}$	electric field intensity vector, V m^{-1}
H	thermoelectric element length, m
h	heat transfer coefficient, W $(K\ m^2)^{-1}$
I	current, A
$\vec{J}$	electric current density vector, A m^{-2}
P	power, W
Pr	price, EUR, €
Q	heat absorbed at the hot junction, W
$\vec{q}$	heat flux vector, W m^{-2}
$\dot{q}$	heat generation rate per unit volume, W m^{-3}
R	internal electrical resistance, Ω
T	temperature, K
ΔT	temperature difference, K
v	voltage, V

Greek symbols

α	Seebeck coefficient, V K^{-1}
ε	dielectric permittivity matrix, F m^{-1}
η	efficiency
λ	thermal conductivity, W m^{-1} K^{-1}
Π	Peltier coefficient, V
ρ	electrical resistivity, Ω m
σ	electrical conductivity, S m^{-1}
φ	electric scalar potential, V

Subscripts

c	cold junction
h	hot junction
n	n-type thermoelectric element
max	maximum
oc	open circuit
opt	optimum
p	p-type thermoelectric element
sc	short circuit

elements are different [9]. For a uni-couple, the footprint area is also important factors in power generation. In an early study, Row and Min [10] studied effect of the TE unit area on power generation for several commercially available modules at the time but with equal footprint area. However, they used constant temperature boundary condition on the cold junction of the modules.

Geometry modification of the TE elements can improve the power generation in the module significantly. Jang et al. [11] explored optimal footprint area of the elements for thin film TEGs and found that the power generation decreases with the area while the efficiency shows different trend.

Chen and Yan [12] attempted to maximize the power generation and efficiency of TEGs by using a model that considers external and internal irreversibility. They determined optimal range of the design parameters. To study the effects of interface layers on TEG module performance, a phenomenological model is applied by Xuan et al. [13] with some simplifications. Using appropriate model also affects the accuracy of the simulation results for thermoelectric elements [14]. A realistic module must consider the thermoelectric phenomena with minimum simplification. Snyder et al. [15] introduced and developed a method called compatibility factor that uses reduce electric current to achieve the highest efficiency determined by figure-of-merit of thermoelectric. Most of the previous theoretical developments are limited to one dimensional models [16] or the TE elements are considered as identical materials so that the differences between thermal and electrical behavior of the TE elements is not accurately evaluated [17]. However there are few studies use computational fluid dynamics simulation environment to evaluate three-dimensional (3D) temperature distribution [18] and to implement TEG model [19] in the thermoelements.

With the tendency of high degree miniaturization in TEG application and due to increase demand of energy recovery, compact TEGs with high density power generation per module volume has been interested. Wang et al. [20] developed a wearable miniaturized TEG. In order to reduce TEG module volume, Whalen et al. [21] designed TEG architecture for more efficient capture of heat from the heat source that can maximize the efficiency and the power density. To improve the volumetric power generation in a TEG, this paper focuses on the key parameter which is thermoelectric element. In this study, parametric optimization of TEG uni-couples is considered in conjunction with practical boundary conditions and with temperature dependent properties of the TE materials. Maximum power generation, maximum cost-efficiency and optimal efficiency in the uni-couples are explored at the matched load condition and over a wide range of n/p footprint area ratios, while the total footprint area of the elements is constant. Moreover, different values of heat transfer coefficient are imposed on the cold junction of uni-couples to consider the effect of thermal boundary condition on the results of the study. The thermoelectrical characteristics of uni-couples are implemented in a 3D simulation environment and are solved by using the finite element method (FEM) and the commercial CFD solver ANSYS-Mechanical APDL. The results of this study are generated based on optimum current through the uni-couples that provides the maximum power in the uni-couples.

2. Governing equations

The TE model in this study, in addition to Seebeck effect, includes Joule heating and Thomson effect. The well-known coupled equations of TE constitutive include both the heat flow and the continuity of electric charge equations [22]:

$$\vec{q} = [\Pi]\cdot\vec{J} - [\lambda]\cdot\nabla T, \tag{1}$$

$$\vec{J} = [\sigma]\cdot(\vec{E} - [\alpha])\cdot\nabla T, \tag{2}$$

$$\vec{D} = [\varepsilon]\cdot\vec{E}, \tag{3}$$

where Eq. (3) is constitutive equation for a dielectric medium. Under steady-state condition, the electric field is irrotational and the coupled equations are in following form [23]:

$$\nabla\cdot([\Pi]\cdot J) - \nabla\cdot([\lambda]\cdot\nabla T) = \dot{q}, \tag{4}$$

$$\nabla\cdot([\sigma]\cdot[\alpha]\cdot\nabla T) + \nabla\cdot([\sigma]\cdot\nabla\varphi) = 0. \tag{5}$$

The heat generation rate per unit volume ($\dot{q}$) in Eq. (4) includes the electric power spent on work against the Seebeck field and on the Joule heating. The open-circuit voltage and the short-circuit current in a TEG uni-couple are as follow:

$$v_{oc} = \overline{\alpha}\Delta T, \tag{6}$$

$$I_{sc} = \frac{\overline{\alpha}\Delta T}{R}, \tag{7}$$

The average Seebeck coefficient of the uni-couple is [24]:

$$\overline{\alpha} = \frac{1}{T_h - T_c}\int_{T_c}^{T_h}(\alpha_p - \alpha_n)dT. \tag{8}$$

The internal resistance of uni-couple in Eq. (7) is as follows [25]:

$$R = R_n + R_p = \left[\left(\sigma_n\frac{A_n}{H_n}\right)^{-1} + \left(\sigma_p\frac{A_p}{H_p}\right)^{-1}\right]. \tag{9}$$

The maximum power generation by the uni-couple can be calculated by an optimal current and electric voltage generation in the uni-couple that happen at half of short-circuit current and half-open circuit voltage. This condition is at the matched load, where the internal electrical resistance of the uni-couple is equal to the imposed electrical load resistance [26,27].

$$P_{max} = v_{opt} \times I_{opt} = \frac{(\Delta T\overline{\alpha})^2}{4R}. \tag{10}$$

The efficiency of the uni-couple is ratio of the power provided to the load and heat absorbed at the hot junction:

$$\eta = \frac{P}{Q}. \tag{11}$$

The length of the studied TE elements is 2 mm, while the footprint area ratios of the squared n/p elements are considered for fifteen cases. Table 1 shows the footprint dimensions of the TE elements with the area ratio of n/p footprints. The total area of the n/p footprints ($A_n + A_p$) is fixed at 8 mm^2 for all the designed uni-couples. The area of the identified ceramic substrate for each TE element is 3 mm × 3 mm; so that the distance between the center points of the TE elements is 3 mm as is shown in Fig. 1. Moreover, Fig. 2 reveals the geometrical design of some sample uni-couples. The thickness of the ceramic substrate and the silver interconnectors are 0.35 mm and 0.25 mm, respectively.

The properties of considered TE materials in this study are temperature dependent. Fig. 3 shows variation of the thermoelectrical properties of the n-type material, $Mg_2Si_{1-x}Sn_x$ [28] and p-type material, Zn_4Sb_3 [29] with temperature. The ceramic substrate is Alumina (AD-995, Nom. 99.5% Al_2O_3) with thermal conductivity of 30 W K^{-1} m^{-1}. The interconnector is Silver with thermal conductivity of 429 W K^{-1} m^{-1}. Electric resistivity variation of the interconnector with the temperature is linear as: $\sigma = (0.0038T + 1.52 \times 10^{-8})$ Ω m [30]. For each stream, the convection heat transfer depends on the flow properties, temperature properties, and fluid type. Typically, the forced convection heat transfer coefficient is in the range of 20–200 W K^{-1} m^{-2} for air and 300–10000 W K^{-1} m^{-2} for water [31]. Therefore, the considered heat transfer coefficients on the cold junction are 50,200,500 and 2000 W K^{-1} m^{-2} in this study. The constant temperature of hot junction is 650 K.

Table 1
Footprint dimensions of the TE elements with the area ratio of n/p thermoelectric elements.

Design no.	D01	D02	D03	D04	D05	D06	D07	D08
A_n/A_p	0.07	0.14	0.23	0.33	0.45	0.60	0.78	1.00
Design no.	D09	D10	D11	D12	D13	D14	D15	
A_n/A_p	1.29	1.67	2.20	3.00	4.33	7.00	15.0	

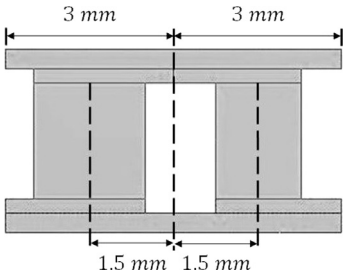

Fig. 1. Side view of a studied uni-couple.

3. Results

A comparison between simulation results in this study and results of 3D numerical models for thermoelectric generators is carried out to valid results of the study. A user defined function introduced by Chen et al. [19] connects TE model to the common CFD simulator FLUENT. The coupled model that is validated by experimental data in order to predict and to optimize the system performance considers a TEG module with 127 uni-couple. The element length is 1.6 mm with cross section area of 1.4 × 1.4 mm^2 for both of the n- and p-type TE elements. In addition, the results of this study are compared with a set of ANSYS couple-field elements [23] with the same material properties that can efficiently and accurately analyze TEGs. The power generation is predicted over wide range of temperature difference between the cold and hot junctions of the uni-couple for a linear load resistance equal to 3.4Ω. The maximum difference between power generation in this study and the power generation in previous studies is 14.2% at the lowest considered temperature different equal to 40 K. Fig. 4 illustrates the good agreement between results of this study and the previous studies [19,23].

The CFD model applied in this study enables the results to demonstrate detailed information of the temperature and potential distribution in the uni-couples. For instance, Fig. 5 illustrates generation of the electric voltage in the uni-couple and the 3D temperature distribution in the model for sample footprint ratio. In contrast to the commonly works on thermoelectricity where the cold junction is at constant temperature, the applied heat transfer coefficients provide realistic thermal boundary condition and shows that the temperature difference between the hot and cold junctions of the TE elements is not the same. This temperature difference is lower in the n-type TE elements compared to the p-type TE element due to the higher thermal conductivity in the n-type material. Therefore, with growth of footprint area of the n-type element, the heat flux across the uni-couple increases as is shown in Fig. 6. As the heat flux is enhanced with increase of the A_n/A_p, the temperature at the cold junction of the elements increases consequently. Therefore, the temperature difference between the hot and cold junctions of the elements decreases.

Although the Seebeck value of the thermoelectric elements increases slightly with the footprint ratio, the voltage generation is dominated by the variation of the temperature difference of the TE elements. Fig. 7 shows the relative variation of the voltage generation at the matched load condition, where at each heat transfer coefficient, the voltage generation of the footprint designs is divided to the voltage generation at D01 as reference footprint ratio. As can be seen, the plots contain an extremum value according to Eq. (6). On the other hand, the variation of the total electrical resistance of the uni-couple has a minimum value due to variation of the footprint area of the n-type and p-type elements. Therefore, there is maximum power generation by the uni-couple (Fig. 8) for a

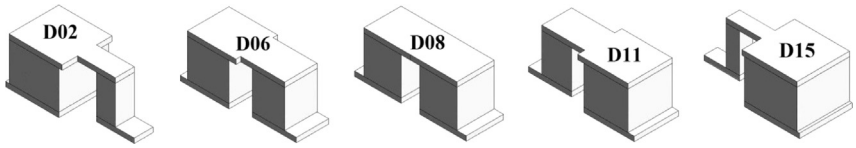

Fig. 2. Sample geometrical designs of the uni-couples.

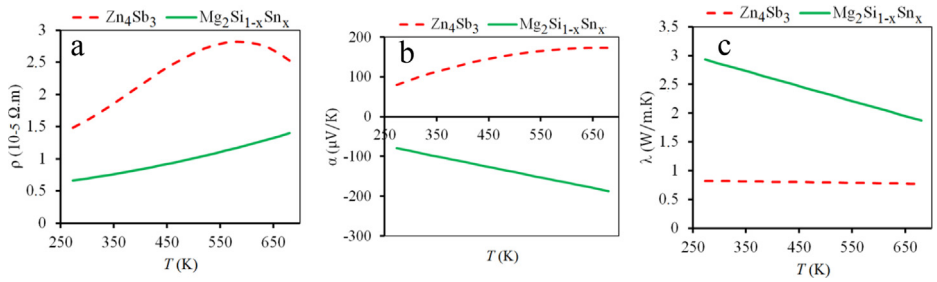

Fig. 3. Variation of thermoelectrical properties of the used TE materials [28,29], (a) electrical resistivity, Ω m, (b) Seebeck coefficient, μV K^{-1}, (c) thermal conductivity, W Ω^{-1} K^{-1}.

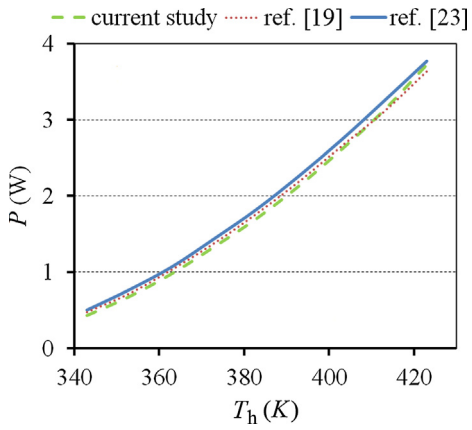

Fig. 4. Comparison of power generation in a TEG module compared with ref. [23] and ref. [19].

constant total footprint area that depends on the thermoelectrical properties of the TE elements and the footprint ratio.

As the A_n/A_p increases, the temperature difference in the elements and therefore the voltage generated in the uni-couple drop with sharper slope at lower heat transfer coefficient. This variation affects the maximum power generation in the uni-couple and shifts it to the larger footprint ratio for higher heat transfer coefficient on the cold junction. However, the minimum electrical resistance is at $A_n/A_p = 0.6$ for all considered heat transfer coefficient in this study. As shown in Fig. 8, the maximum power generations occur at A_n/A_p = 0.23,0.33,0.45,0.6, for h_c = 50,200,500,2000 W K^{-1} m^{-2}, respectively. The results show that the optimal footprint ratio not only follows the electrical resistance of the uni-couple, it also is dependent to the thermal boundary condition, specifically at lower values of the heat transfer coefficient. The conversion efficiency of the uni-couple at matched load condition is also affected by the footprint ratio, so that the increase of the heat flow across the uni-couple with the A_n/A_p shifts the maximum efficiency to smaller footprint ratio. According to the (12), Fig. 9 shows the variation of efficiency with the footprint ratio where the maximum efficiency happens at A_n/A_p = 0.14,0.23,0.33,0.33, for h_c = 50,200,500, 2000 W K^{-1} m^{-2}, respectively.

To design a cost effective TEG module, not only the optimal footprint ratio must be considered, the cost to provide an effective heat transfer coefficient for optimal design of the heat sink and also a comparison of the material cost should be considered. Increase in the heat transfer coefficient required higher pumping power that decreases the net power by the module. In this study, density of the considered n-type and p-type TE materials are 3000 and6400 kg m^{-3} with assumed price of Pr = 100 and 200 € kg^{-1}, respectively. These prices are estimated based on raw materials without consideration of process cost. Although, actual costs depend on the scale of production and procedures of synthesis, the overall cost of the compounds will be close to the assumed amounts for large scale production processes. The variation of ratio

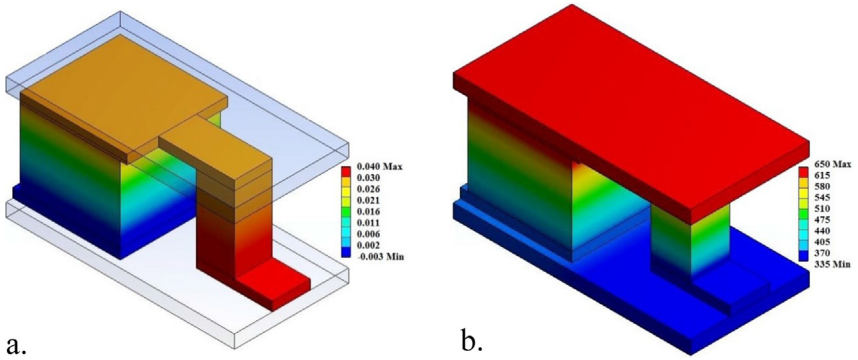

Fig. 5. a. generation of the electric voltage, b. 3D temperature distribution in the uni-couple, A_n/A_p = 6.97, h_c = 2000 W K^{-1} m^{-2}.

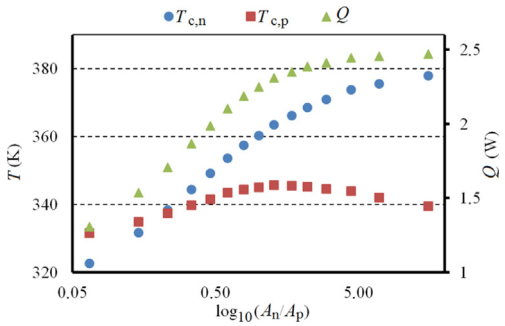

Fig. 6. Cold junction temperature of the TE elements and hot junction heat absorbed, $h_c = 2000$ W K^{-1} m^{-2}.

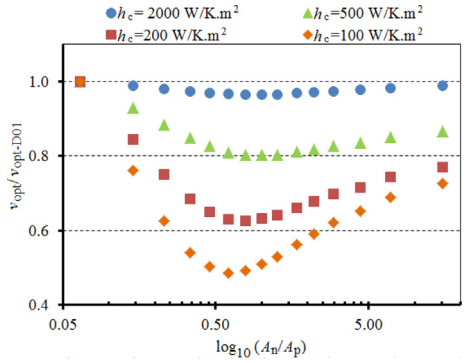

Fig. 7. Relative variation of the voltage generation at the matched load condition.

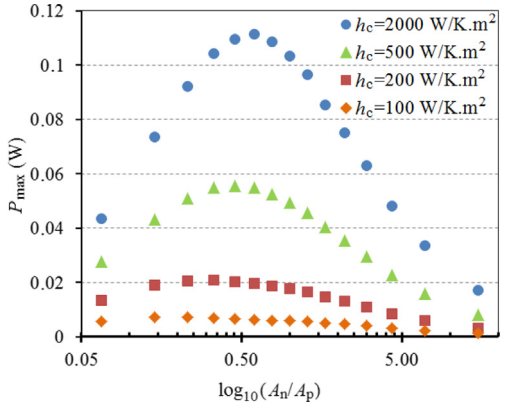

Fig. 8. Maximum power generation by the uni-couple with variation of the footprint ratio.

of the maximum power generation to the cost of the TE materials with the footprint ratio shows that the maximum cost-efficiency (W/€) in this study happens at lower footprint ratio compared to the maximum power generation and maximum efficiency at the matched load condition.

4. Conclusions

This study explores optimum footprint ratio of the n- and p-type TE elements with temperature dependent thermoelectrical properties of the materials. The 3D governing equations of thermoelectricity are solved using the FEM, and the analysis of the model generates detailed description of the temperature distribution and voltage generation in the uni-couples by using realistic thermal boundary conditions. The results illustrates that the maximum

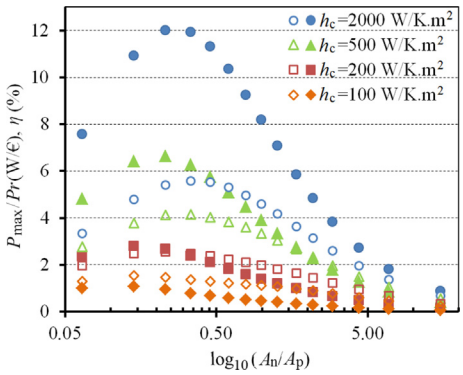

Fig. 9. Variation of efficiency and cost-efficiency with the footprint ratio, ●▲■◆P_{max}/Pr, ○△□◇ η(%).

power generation occurs where $A_n/A_p < 1$ due to lower electrical resistance and higher thermal conductivity of the n-type TE materials considered in current study. The results also show that, the maximum power generation occurs at smaller footprint ratio when the heat transfer coefficient on the cold junction decreases. Since the footprint area of the n- and p-type TE elements are mostly equal in commercial TEG modules, the proposed optimization aids to reduce TE material consumption in the optimal modules. This study demonstrates optimal footprint ratio for applications of the maximum power generation and maximum performance per price of the TEG modules.

Acknowledgments

This work was carried out within the framework of the Center for Energy Materials and is funded in part by the Danish Council for Strategic Research, Programme Commission on Energy and Environment, under Grant No. 823032.

References

[1] B.I. Ismail, W.H. Ahmed, Recent Pat. Electr. Eng. 2 (2009) 27–39.
[2] S. Fiameni, S. Battiston, S. Boldrini, A. Famengo, F. Agresti, S. Barison, M. Fabrizio, J. Solid State Chem. 193 (2012) 142–146.
[3] D. Zhang, F. Yan, T. Shimotori, K.C. Wang, Y. Huang, J. Power Sources 217 (2012) 65–71.
[4] C.C. Weng, M.J. Huang, Int. J. Therm. Sci. 71 (2013) 302–309.
[5] Y. Wang, C. Dai, S. Wang, Appl. Energy 112 (2013) 1171–1180.
[6] R.C. O'Brien, R.M. Ambrosi, N.P. Bannister, S.D. Howe, H.V. Atkinson, J. Nucl. Mater. 377 (2008) 506–521.
[7] K. Yazawa, A. Shakouri, Environ. Sci. Technol. 45 (2011) 7548–7553.
[8] A. Rezania, K. Yazawa, L.A. Rosendahl, A. Shakouri, Int. J. Therm. Sci. 72 (2013) 73–81.
[9] Y. Wang, X. Zhang, L. Shen, N. Bao, C. Wan, N.H. Park, K. Koumoto, A. Gupta, J. Power Sources 241 (2013) 255–258.
[10] D.M. Row, G. Min, J. Power Sources 73 (1998) 193–198.
[11] B. Jang, S. Han, J.Y. Kim, Microelectron. Eng. 88 (2011) 775–778.
[12] J. Chen, Z. Yan, L. Wu, J. Appl. Phys. 79 (1996) 8823–8828.
[13] X.C. Xuan, K.C. Ng, C. Yap, H.T. Chua, Int. J. Heat Mass Transfer 45 (2002) 5159–5170.
[14] G. Fraisse, J. Ramousse, D. Sgorlon, C. Goupil, Energy Convers. Manage. 65 (2013) 351–356.
[15] G.J. Snyder, in: D.M. Rowe (Ed.), Thermoelectrics Handbook Macro to Nano, Taylor & Francis, 2006. Section 9.6.4, (Chapter 9).
[16] A.J. Minnich, M.S. Dresselhaus, Z.F. Ren, G. Chen, Energy Environ. Sci. 2 (2009) 466–479.
[17] J.Y. Jang, Y.C. Tsai, Appl. Therm. Eng. 51 (2013) 677–689.
[18] A. Rezania, L.A. Rosendahl, J. Electron. Mater. 41 (2012) 1298–1304.
[19] M. Chen, L.A. Rosendahl, T. Condra, Int. J. Heat Mass Transfer 54 (2011) 345–355.
[20] Z. Wang, V. Leonov, P. Fiorini, C. Van Hoof, Sens. Actuators 156 (2009) 95–102.
[21] S.A. Whalen, C.A. Apblett, T.L. Aselage, J. Power Sources 180 (2008) 657–663.
[22] L.D. Landau, E.M. Lifshitz, Electrodynamics of Continuous Media, second ed., Butterworth-Heinemann, Oxford (, 1984.
[23] E.E. Antonova, D.C. Looman, in: 24th International Conference on Thermoelectrics, 2005, pp. 215–218.

[24] R. Decher, Direct Energy Conversion – Fundamentals of Electric Power Production, Oxford University Press, Inc., 198 Madison Avenue, New York, 1997.
[25] A. Bitschi, Modelling of Thermoelectric Devices for Electric Power Generation (PhD Theses), Swiss Federal Institute of Technology, Zurich, Swiss, 2009. No. 18441.
[26] F.J. Lesage, N. Pagé-Potvin, Energy Convers. Manage. 66 (2013) 98–105.
[27] F.J. Lesage, R. Pelletier, L. Fournier, É.V. Sempels, Energy Convers. Manage. 74 (2013) 51–59.
[28] M. Sondergaard, M. Christensen, K.A. Borup, H. Yin, B.B. Iversen, Acta Mater. 60 (2012) 5745–5751.
[29] H. Yin, S. Johnsen, K.A. Borup, K. Kato, M. Takatac, B.B. Iversen, Chem. Commun. 49 (2013) 6540–6542.
[30] R.A. Serway, Principles of Physics, second ed., Saunders College Publishing, Fort Worth, Texas; London, 1998, p. 602.
[31] C. Lasance, C. Moffat, Electron. Cool. 11 (2005).